
Araştırma Makalesi / Research Article

A Battery Management System Design Including a SOC Estimation Approach for Lead-Acid Batteries

Emre AKARSLAN^{1*}, Said Mahmut ÇINAR²

¹ Afyon Kocatepe Üniversitesi, Mühendislik Fakültesi, Elektrik Mühendisliği Bölümü, Afyonkarahisar, Türkiye,
ORCID ID: <https://orcid.org/0000-0002-5918-7266>, akarslan@aku.edu.tr

² Afyon Kocatepe Üniversitesi, Mühendislik Fakültesi, Elektrik Mühendisliği Bölümü, Afyonkarahisar, Türkiye,
ORCID ID: <https://orcid.org/0000-0002-6810-1575>, smcinar@aku.edu.tr

Geliş/ Received: 24.10.2022;

Kabul / Accepted: 08.12.2022

ABSTRACT: Storage is one of the most important issues of the last decades. In particular, storage systems are needed in order to benefit more effectively from renewable energy systems where production cannot be controlled. One of the most important problems in storage is that as the amount of energy desired to be stored increases, the need for space also increases. Therefore, it is of great importance to manage energy effectively in such systems. In this study, a battery management system (BMS) that can be used for lead acid batteries has been designed. This BMS has a measurement and control system based on STM 32 microcontroller and is controlled via an interface prepared in the MATLAB Simulink environment and the test data is imported into the MATLAB Workspace environment. The designed system can also perform battery charge-discharge experiments in accordance with the battery characteristics. Charge-discharge experiments were carried out using the designed system, and a model was developed to determine the state of charge (SOC) of the battery using the data collected during these experiments. With the model developed based on Elman Neural Networks, the SOC of battery could be estimated at an error level of less than 1%.

Keywords: Battery Management System (BMS), State of Charge (SOC), Elman Neural Network.

*Sorumlu yazar / Corresponding author: akarslan@aku.edu.tr

Bu makaleye atıf yapmak için /To cite this article

Akarslan, E., Çınar, S. M., (2022). A Battery Management System Design Including a SOC Estimation Approach for Lead-Acid Batteries. Journal of Materials and Mechatronics: A (JournalMM), 3(2), 300-313.

1. INTRODUCTION

The depletion of fossil fuel resources, the energy crisis and global warming have motivated the development of clean energy for electricity generation and smart grids (Hossain Lipu et al., 2021; Ansari et al., 2022). In addition, renewable energy sources come to the fore in this period due to their sustainability and the realization of consumption at the point of production. Among these renewable resources, solar and wind are the most scalable methods of producing clean energy (Zhao et al., 2020). Since the availability of solar and wind energy depends on weather conditions, it becomes difficult to manage the grid, so it becomes essential to develop strategies to ensure uninterrupted supply and develop energy storage systems (Tawalbeh et al., 2022). Lead acid batteries are frequently used in various areas, such as renewable energy systems, uninterruptible power systems, etc., since they are inexpensive, safe, and require less maintenance (Somasundaram et al., 2022). As with all battery types, these batteries should be observed and kept under control when used together. For this purpose, battery management systems (BMS) are used. The BMS is like a brain that monitors and controls parameters such as the cell's current, voltage, and temperatures to prevent damage and deterioration of cells and to extend the cell's life span by keeping it within safe operating ranges (Ren et al., 2019). Batteries are used in many areas, such as portable electronic devices, electric vehicles, smart grids, and battery management systems are needed for safe and effective use. A BMS can undertake a wide variety of tasks such as input/output current and voltage monitoring, charge-discharge control, inter-cell charge balancing, prediction of battery health, prediction of battery charge status, battery protection, and fault diagnosis (Cui et al., 2022; Corkhuff et al., 2018). One of the main tasks of the BMS is to accurately determine the state of charge (SOC) of the battery. The battery's SOC reflects its remaining power. In this context, accurate SOC estimation can improve battery efficiency, extend service life, and ensure battery reliability and safety (Wu et al., 2022; Lv et al., 2021). There are many studies in this field in the literature.

Ren et al. (2019) design a BMS to monitor and control the battery's temperature, SOC and state of health (SOH), thereby increasing the efficiency of rechargeable batteries. In the study, lithium-ion batteries were used for storage, and an active balancing system was preferred. In the study, the battery's remaining capacity was estimated based on each cell terminal voltage measurement. In the balancing process, the output voltage ripples are taken under control by taking into account the SOC estimates. Experimental results show that output voltage ripples can be minimized with more accurate SOC estimations (Ren et al., 2019). Okay et al. (2022) develop a prototype BMS for a grid-connected residential-photovoltaic (PV) system with lithium-ion batteries. It provides safe operation conditions by monitoring and controlling the battery parameters during the charge/discharge process. Furthermore, the BMS manages the energy flow between the PV system, battery, grid, and load (Okay et al., 2021). Liu and Yu (2022) use the square root unscented Kalman filter (SR-UKF) method for SOC estimation on lithium cobalt oxide batteries. They also construct a MATLAB/Simulink model for evaluating experimental results with less than 25 mV error. The experimental results show that more successful results were obtained with the SR_UKF model than with the traditional Kalman filter model (Liu and Yu, 2022). Jin et al. (2021) develop a second-order RC equivalent circuit model for lithium-ion batteries which considers the influence of discharge rate. An extended Kalman filter (EKF) model is employed for SOC estimation. Experiments show that under the condition of intermittent pulse discharge with gradually decreasing amplitude, the precision of estimating SOC can be significantly improved using the proposed approach (Jin et al., 2021). Cui et al. (2022)

construct the Thevenin equivalent circuit model of lithium-ion batteries. The extended Kalman filter approach is used for SOC estimation, and it is shown that this approach eliminates the Gaussian error. A test system is constructed in MATLAB/Simulink environment, and the performance tests are shown that a better performance is achieved than the traditional one (Cui et al., 2022). Singh et al. (2020) propose a model for SOC estimation. The model is utilized from the coulomb counting method, open circuit voltages, and ANFIS, and the effect of the temperature is also considered. The superiority of the proposed method has been demonstrated by experiments carried out under the same load conditions in a laboratory environment (Singh et al., 2020). Kuchly et al. (2021) propose using neural networks in the SOC estimation of a lithium-ion battery. Unlike the existing literature, the past-past current integral is used as input instead of instantaneous information in the proposed method. The results of the presented study revealed the success of artificial neural networks in SOC prediction (Kuchly et al., 2021).

In this study, Lead-acid batteries are selected since these kinds of batteries are preferred in uninterrupted power supplies and renewable energy systems. Serial-connected three 12 V 7 Ah Valve Regulated Lead Acid (VRLA) batteries are used in the experiments. A BMS based on STM32 microcontroller is designed. It is aimed to design a battery management system based on STM microcontroller. The designed BMS can carry out charge-discharge experiments according to battery characteristics and observe parameters such as current, voltage, and temperature during the experiments. Furthermore, passive balancing can be done with the designed system to ensure battery safety. In this scope, several experiments are performed, and parameters are collected. In the second part of the study, the Elman Neural Network based model is constructed for battery SOC estimation in a computer environment using collected data via an embedded system. The experimental results revealed the success of the proposed model.

2. THE EXPERIMENTAL SETUP

The experiment platform consists of a microcontroller development board, personal computer (PC), control board, test batteries, balancing resistors, discharge resistors, and power supply (Figure 1). At the center of the experimental platform is an STM32 Discovery F4 development board. The development board is connected to the PC via two USB ports that perform debugging and data transfer functions. On the control card, some relays controlled balancing resistors and charge-discharge phases, and current, voltage, and temperature sensors conditioning circuits are taken part. In addition, there are suitable terminals for power supply, batteries, temperature sensors, balancing resistors and discharge resistors, power supply connections, and connectors where the cables connecting to the development board are attached. The tested batteries consist of three cells, and the cell temperatures are sensed by the LM35 device attached to the bodies of the batteries. The firmware and user interface are graphically designed in the MATLAB Simulink environment. These components of the experimental setup are detailed below.

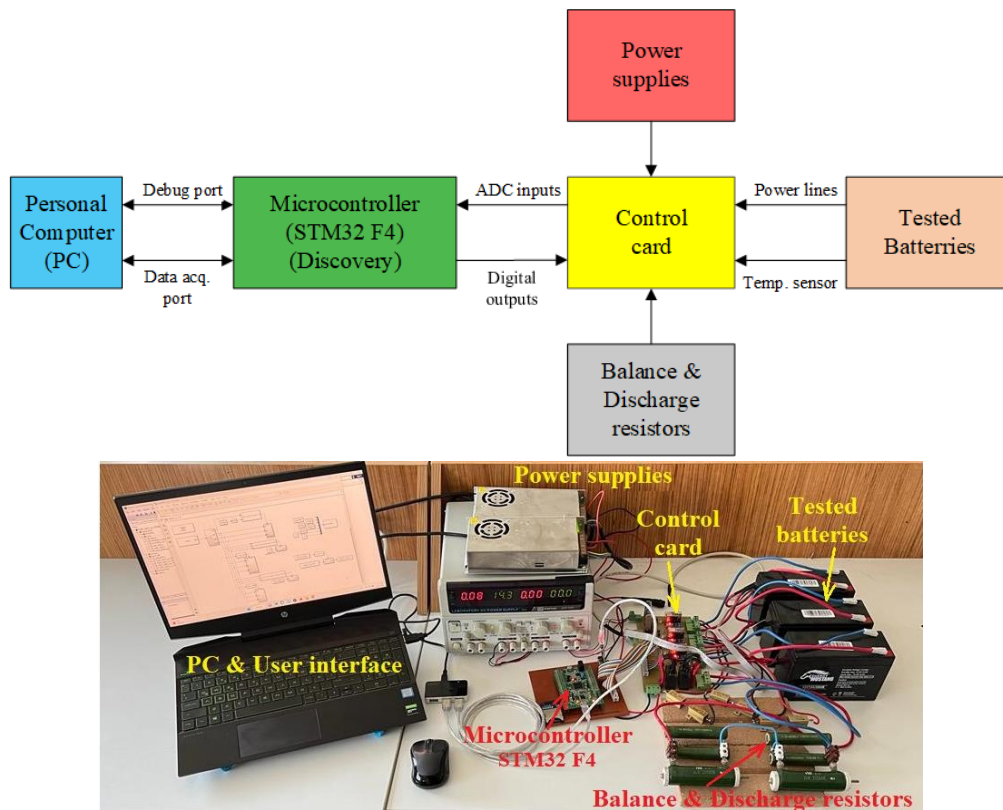


Figure 1. Block diagram of experimental setup

1. Development card and designed expansion shield:

STM32 Discovery-F4 development board has a microcontroller based on ARM Cortex M4 series STM32F407VGT6. The development board also has an ST-LINK/V2-A debugging unit that can be used for programming and debugging the microcontroller. The development board is attached in an expansion shield designed for this study (Figure 2). This shield has two connectors for digital and analog signals, one serial communication ports terminal, and an SD card module. In addition, low-pass filters were added to analog input ports.

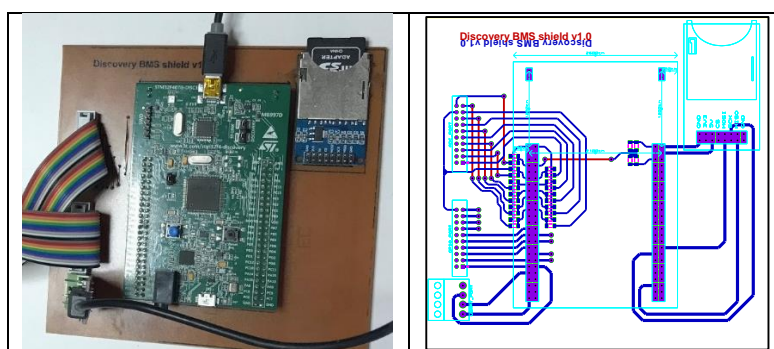


Figure 2. Designed expansion shield for STM32 Discovery-F4

2. The control and measurement card:

The control card is sized to fulfill the power control and measurement tasks of three battery cells. The connections between the power control and measurement card and the expansion card are designed to provide electrical isolation. For this purpose, ACS712 series hall-effect based current sensors are used for current measurements, while ACPL series optical insulation-based voltage sensors are used for voltage measurements. In industrial/real applications, although an insulation

standard is not observed as much as in the measuring circuits used in this study, it has been tried to establish a high insulation standard in this presented R&D study. In addition, relays are used to initiate the charge or discharge phases and to activate and deactivate passive balancing resistors. Thus, any high voltage transitions from the power stage that may disrupt the micro-controller inputs or outputs can be prevented. A view of the power control and measurement board of the designed BMS is presented in Figure 3.

3. Firmware software:

The microcontroller's firmware was designed model-based, and for this, MATLAB Code generation, Simulink plugins, IAR Embedded Workbench development, and STM32CubeMx configuration software were used. This firmware performs many functions, such as managing the sampling times of analog signals from current, voltage, and temperature sensors, controlling balancing resistors, starting and stopping the charge and discharge phases, and data transfer via the user interface.

In the firmware design, the microcontroller is firstly configured on STM32CubeMx software (Figure 4). The general purpose input-output (GPIO) pins, an analog-digital converter (ADC), timers, and universal synchronous-asynchronous receive transmit (USART) peripheral modules are configured with the software, and a configuration file (*.ioc) is created. The configuration determines many design parameters, such as ADC channel sampling times, interrupt timing, direct memory access (DMA) dimension, USART baud rate, and DMA receive-transmit buffer dimension.

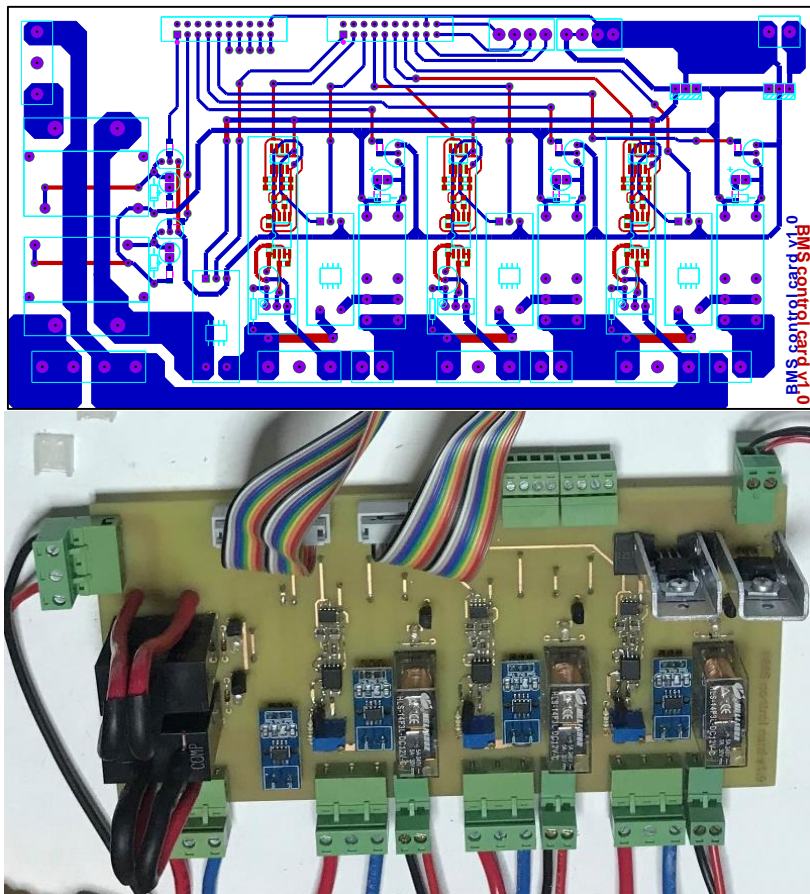


Figure 3. Designed control card

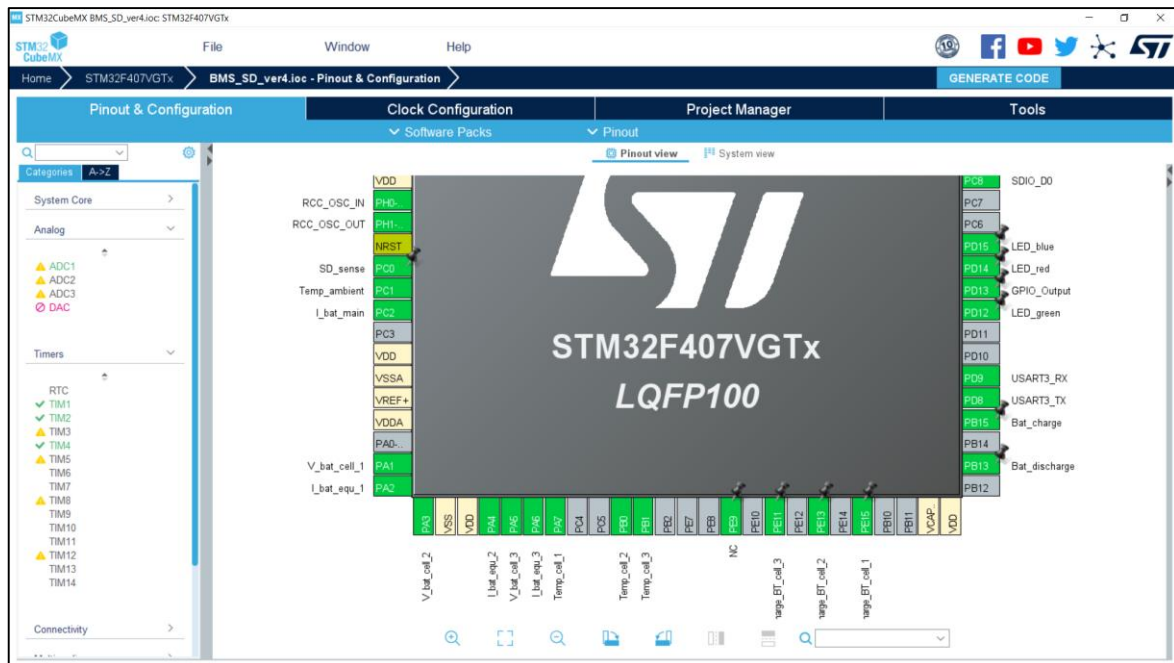


Figure 4. The microcontroller configuration software

After producing the configuration file, ADC sampling, ADC processing, USART sending and receiving, and battery equalizing tasks are programmed as model based in MATLAB/Simulink environment (Figure 5). In the study, the ADC sampling time is set to 4 milliseconds (ms), and ADC results are buffered with the DMA unit. After the buffer is full (total 128x11 words) root mean square (RMS) value of each channel is computed and sent via the USART. The data-packed, which includes the GPIO output logic levels produced by the BMS algorithm operated in the user interface and sent over the serial port at 500 ms intervals, are met with the USART data receive interrupt and buffered with DMA. Finally, the outputs are driven according to receiving data via USART.

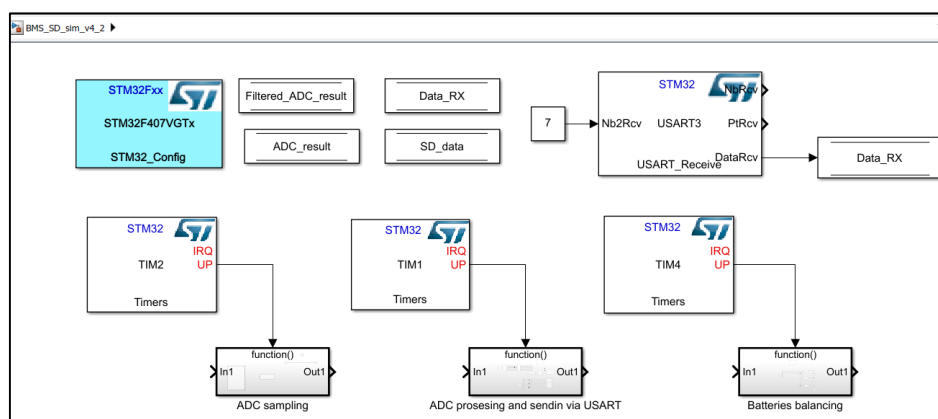


Figure 5. The model-based firmware design

The model prepared in the MATLAB/Simulink environment is built with the Code Generation tool, and C codes compatible with the IAR compiler are created (Figure 6). This way, C codes are produced effortlessly, and prototyping times can be considerably shortened. The generated code can be embedded in the microcontroller via the ST-LINK debug port, and debugging can be performed on the IAR-embedded workbench.

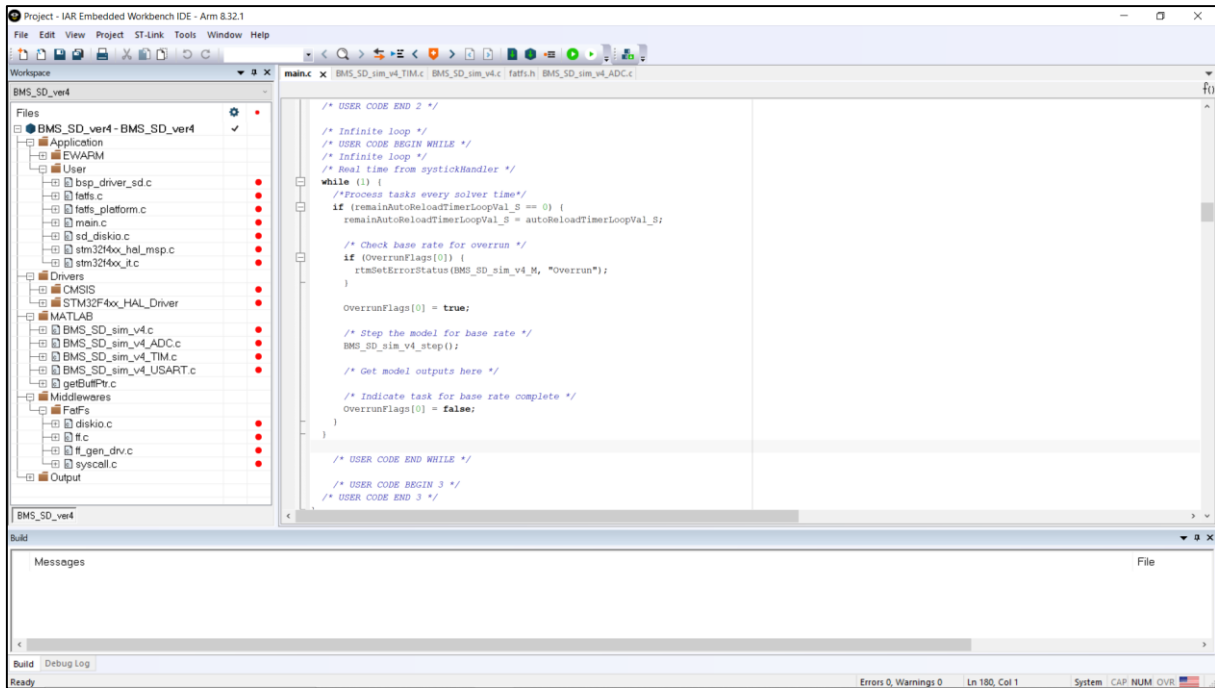


Figure 6. IAR integrated development environment.

4. User interface:

The main function of the user interface (Figure 7) is to display and store the test results. In this application, however, the initiation of the charge and discharge phases and the operation of the BMS passive balancing algorithm are also performed in the user interface. It is considered that these algorithms will be embedded in the firmware in the future. The Cortex M4 series microcontroller used in the study has 1MB flash program memory and 192+4KB RAM memory capacity, which can operate up to 168 MHz. Therefore, when the BMS algorithm running on the interface is embedded in the microcontroller, the algorithm can be run in real-time without any problems.

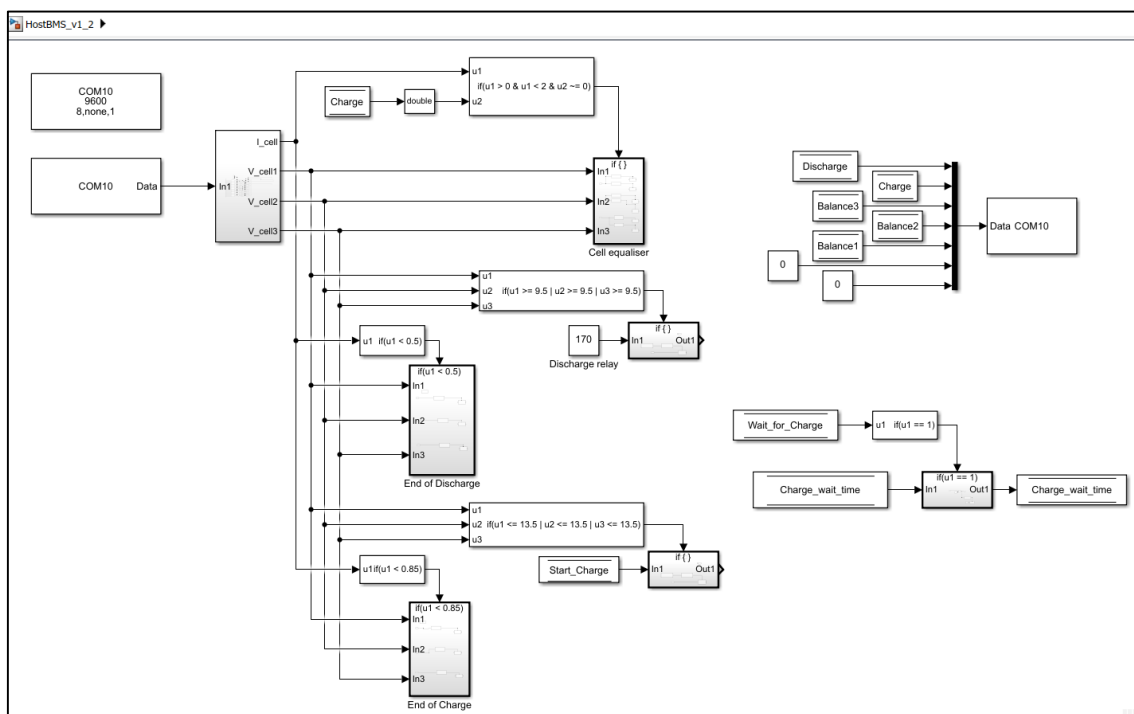


Figure 7. User interface for BMS

3. ELMAN NEURAL NETWORKS

In this study, Elman Neural Network is used for SOC estimation of Lead Acid Batteries. Elman neural network is a dynamic recurrent network proposed by J. L. Elman for solving a signal processing problem (Akarslan, 2022; Elman, 1990). Unlike other types of neural networks, it has a load-bearing layer and therefore provides a better prediction performance (Zhao et al., 2020). The input layer node acts as a signal transmission, while the output layer node works as a linear weight function. A linear or non-linear transfer function can be used in the hidden layer node. The previous value of the hidden layer can be hidden by the additional context layer, called one-step time delays (Zhang et al., 2019). In training, the context layer receives the feedback signal from the hidden layer and puts the previous output of the hidden layer into its input via the memory link. The basic schematic view of ENN is presented in Figure 8. In this study, battery voltage, temperature, and main branch current values are used as inputs for Elman Neural Network, and the network's output is the battery state of charge (SOC).

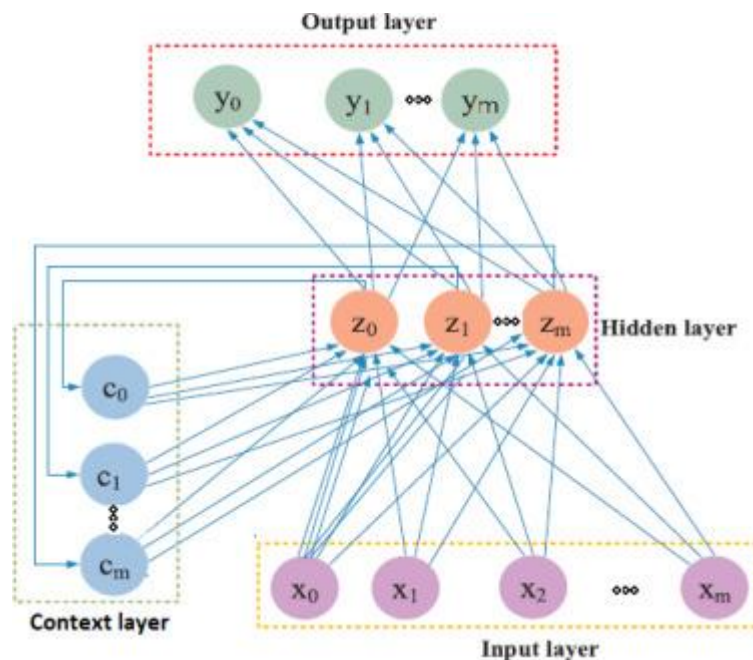


Figure 8. The principle schema of the Elman neural network (Li et al., 2018)

4. EXPERIMENTAL RESULTS

In this study serial connected three 12 V 7 Ah VRLA battery system is used for experiments, and a BMS system is designed. The designed BMS has some abilities, such as performing charge-discharge experiments, collecting current, voltage, and temperature data, providing passive balancing, etc. In this scope, the abilities of the designed BMS are tested. By using designed system, the data set containing 11 time series related to the current, voltage, temperature and ambient temperature of the battery cells is transferred to the MATLAB Workspace screen (Figure 9).

This figure also shows a time graph of the battery voltage in the charge-discharge cycle of the battery. While the battery is being discharged in the first part of the graph (in this part, a linear decrease in voltage is observed since the battery is discharged under constant load in this part), it is charged in the second part. In the charging part, after a sudden increase in voltage is observed with the start of charging, it is observed that the voltage increases almost linearly. In the last part of the

graph, fluctuations in voltage can be seen. This section shows that the passive balancing system is activated.

Figure 10 illustrates the variation of main branch current with time. In the discharge phase, it is seen that the current that can be drawn from the battery decreases over time, while the current drawn by the battery in the charging phase remains constant for a long time. This is provided by the BMS (in accordance with the battery characteristic). It was stated in the battery endurance that it would be appropriate for the battery to draw a maximum current of 2.1 A during charging, and this was also provided by BMS. Figure 5 illustrates the temperature variations in different experiments.

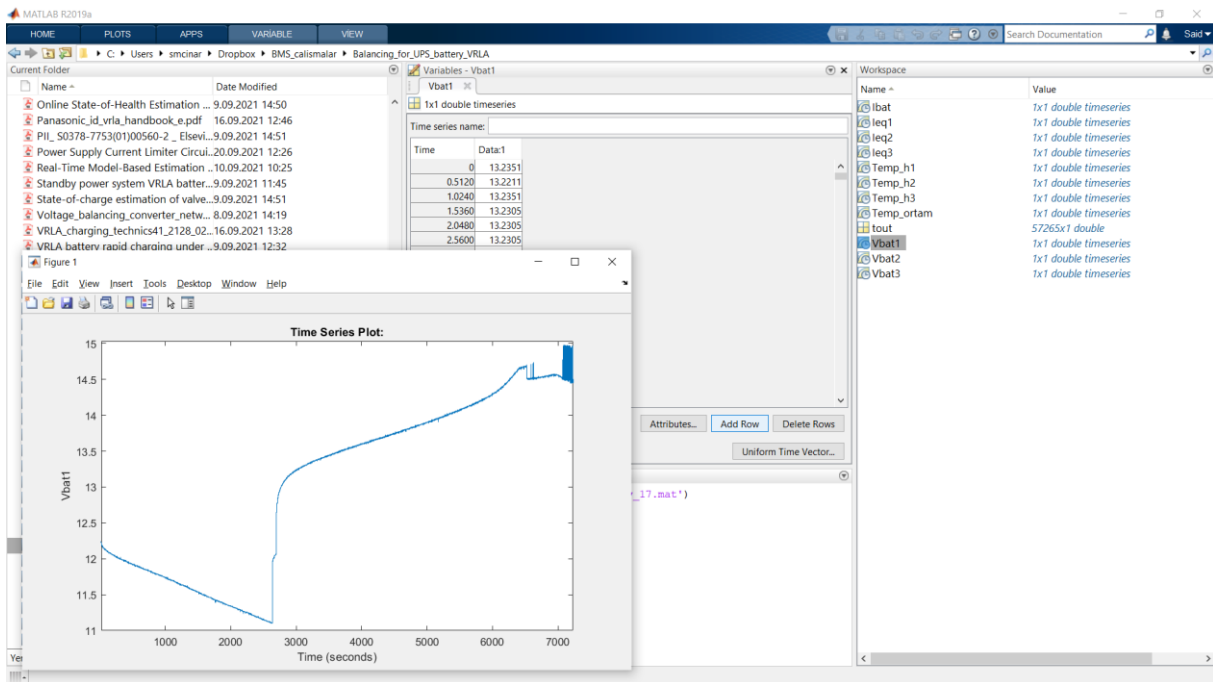


Figure 9. A view of the MATLAB workspace screen with experimental data

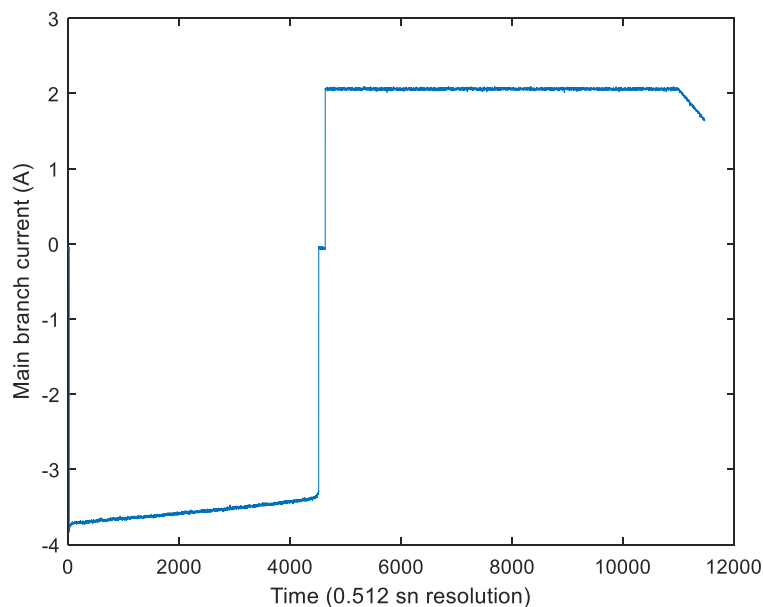


Figure 10. Time graph of main branch current in a discharge-charge cycle

In the study, two charge-discharge cycle experiments were carried out every day, and the graphs in the same color in this figure show the experiments performed on the same day. In the experiments carried out, there is no mechanism to keep the temperature constant, and it is seen that the temperature increases over time (Figure 11). This effect of temperature was also taken into account when evaluating the results. The results mentioned so far show that the state of charge of the battery is related to the current, voltage and temperature values of the battery. For this reason, an Elman neural network model was developed to predict the state of charge of the battery using the three mentioned parameters as inputs.

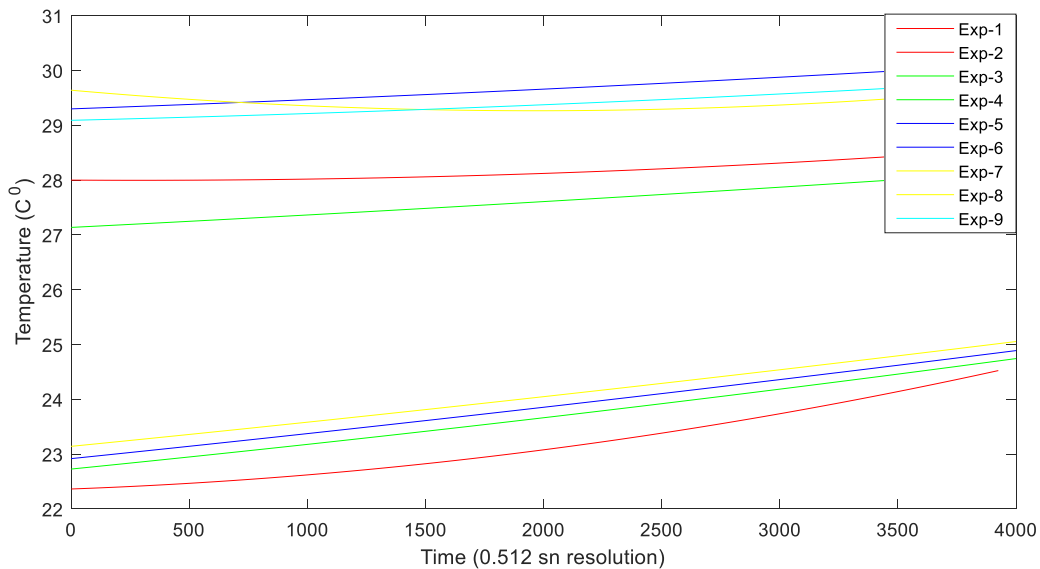


Figure 11. Temperature values observed in the discharge phase of a battery in different experiments

In this context, the data of 12 experiments out of the data of 18 experiments were used in training, and data from 6 experiments were used in the testing phase. Since three battery cells of the same model were used in the experimental setup, the SOC value is estimated for any battery cell at any time, regardless of which battery cell it belongs to, using the specified parameters. However, in order to compare their performance, the performance of the model created in the case of only charging, only discharging, and using all values without knowing which phase they belong to, as mentioned above, is examined. In the created Elman Neural Network, after various trials, it was decided to have two hidden layers and six and eight neurons in these layers, respectively. While tansig and logsig activation functions are used in the hidden layer, the linear activation function is used in the output layer. The variation graph of error in the training phase for the Elman Neural Network is illustrated in Figure 12. In Table 1, the performance values for the estimations in the case of only the charge phase data, only the discharge phase data, and all data are presented.

Table 1. Performance results on SOC estimation

	RMSE	RMSE(%)	MBE	r	r2
Discharge	0.2885	0.61	-0.003	0.9993	0.9986
Charge	0.2879	0.47	-0.0019	0.9995	0.999
Both (C/D)	0.2983	0.53	0.002	0.9996	0.9992

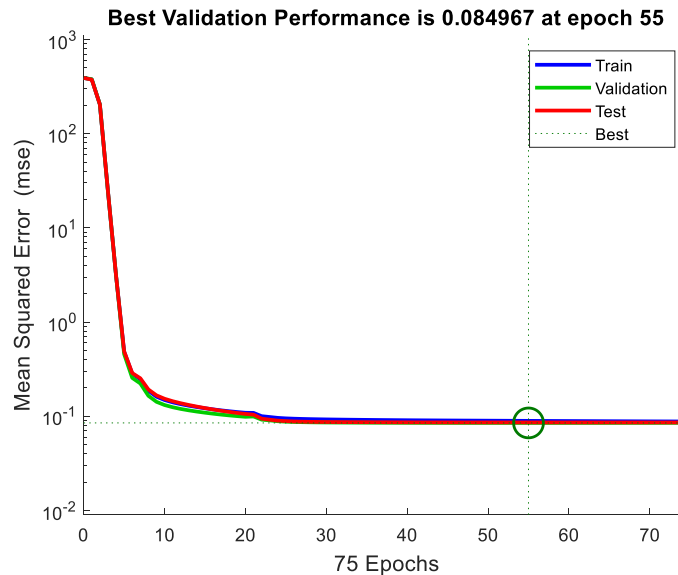


Figure 12. Variation graph of error in training phase for Elman Neural Network

The Root Mean Square Error (RMSE), Mean Bias Error (MBE), correlation coefficient (r), and specificity coefficient (r^2) parameters are used as performance criteria. When Table 1 is examined, it is seen that the RMSE value in the SOC estimation is 0.2983 when all data are used. In order to see what this value is compared to the size of the data in the data set, the percentile RMSE value was also calculated and the error was determined to be 0.53%. It shows that quite successful predictions were made. The MBE value was determined as 0.002, which indicates that these estimates are quite balanced. It is seen that the correlation and specificity coefficients are at the level of 0.99. The closeness of these values to 1 reveals the success of the estimation. Figure 13 shows the correlation graph between the actual and predicted values for all data. As seen from the figure, the data were collected on the diagonal axis, indicating the prediction's success.

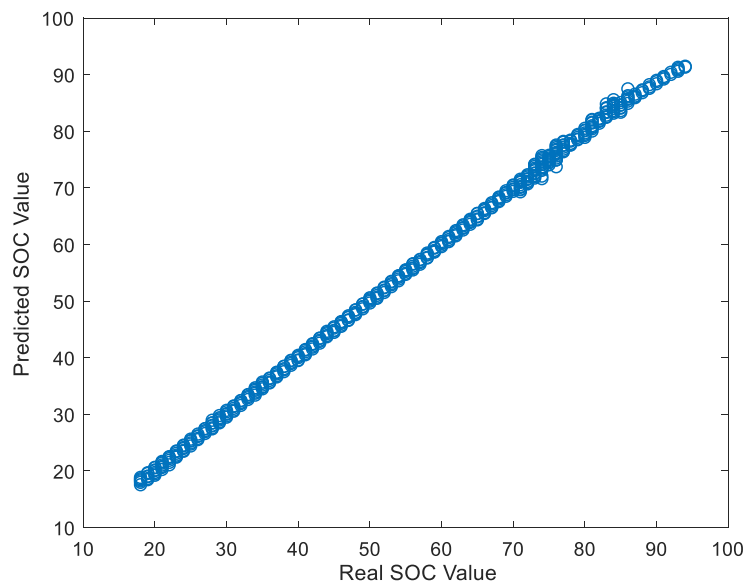


Figure 13. Correlation graph of actual values and predicted values

In order to compare the results obtained from the study with the existing studies, the results obtained from various methods used in the literature are presented in Table 2. When Table 2 is examined, it is seen that very successful estimations are made with the approach used in the study.

Table 2. SOC estimation error comparison

Method	Battery Type	RMSE (%)
Linear Matrix Inequalities (Shen and Rahn, 2013)	Lead- Acid	4.93
Switched Model (Shen and Rahn, 2013)	Lead- Acid	0.35
Dynamic data-driven (Li et al., 2016)	Lead- Acid	2.08
Extended Kalman Filter (Wang et al., 2017)	Li-ion	1.33
Elman Neural Network (This study)	Lead- Acid	0.2983

5. CONCLUSION

In this study, it was aimed and realized to design an STM-based battery management system. The developed BMS has features such as carrying out charge-discharge experiments, controlling the charge-discharging process in accordance with the battery characteristics, observing and recording parameters such as current, voltage, and temperature during the experiments, and protecting the system in case the measured parameters go out of the determined limits. In addition, the designed BMS is capable of passive balancing. The designed BMS was tested on a system with three lead acid batteries connected in series. In the first part of the study, the ability of the BMS to fulfill the desired features was tested and it was observed that the desired features were provided. The designed system can be controlled via a computer, or the system can operate independently of the computer. In the second step, an Elman Neural Networks-based prediction model was created that can predict the battery state of charge at any time by determining the parameters related to the state of charge of the battery. The current, voltage, and temperature data of the batteries are selected as features and used as inputs of the algorithm. The test results show that the state of charge of the battery can be predicted with errors less than 1%. In the presented study, the SOC prediction process is executed on computer using data from the embedded system. It is planned as a future study to carry out the whole process in the embedded system, including the SOC estimation.

6. ACKNOWLEDGEMENTS

This study was supported by Afyon Kocatepe University Scientific Research Projects Coordination Unit with Project number of 18. KARIYER.193.

7. CONFLICT OF INTEREST

Authors approve that to the best of their knowledge, there is not any conflict of interest or common interest with an institution/organization or a person that may affect the review process of the paper.

8. AUTHOR CONTRIBUTION

Emre AKARSLAN; determining the concept and design process of the research, data analysis, writing, experimental studies, and interpretation of results. Said Mahmut ÇINAR; determining the

concept and design process of the research, experimental studies, data collection and analysis, and interpretation of results.

9. REFERENCES

- Akarslan E., Learning Vector Quantization based predictor model selection for hourly load demand forecasting, *Applied Soft Computing* 117, 108421, 2022. <https://doi.org/10.1016/J.ASOC.2022.108421>.
- Ansari S., Ayob A., Hossain Lipu M. S., Hussain A., Md Saad M. H., Remaining useful life prediction for lithium-ion battery storage system: A comprehensive review of methods, key factors, issues and future outlook. *Energy Reports* 8, 12153-12185, 2022. <https://doi.org/10.1016/j.egyr.2022.09.043>
- Carkhuff B. G., Demirev P. A., Srinivasan R., Impedance-Based Battery Management System for Safety Monitoring of Lithium-Ion Batteries. *IEEE Trans Ind Electron* 65, 6497-6504, 2018. <https://doi.org/10.1109/TIE.2017.2786199>.
- Cui Y., Lin K., Zhu J., Chen Y., Quantum-inspired degradation modeling and reliability evaluation of battery management system for electric vehicles. *Journal of Energy Storage* 52, 104840, 2022. <https://doi.org/10.1016/J.EST.2022.104840>.
- Cui Z., Hu W., Zhang G., Zhang Z., Chen Z., An extended Kalman filter based SOC estimation method for Li-ion battery. *Energy Reports* 8(5), 81-87, 2022. <https://doi.org/10.1016/J.EGYR.2022.02.116>.
- Elman J. L., Finding structure in time. *Cognitive Science* 14(2), 179-211, 1990. [https://doi.org/10.1016/0364-0213\(90\)90002-E](https://doi.org/10.1016/0364-0213(90)90002-E).
- Hossain Lipu M. S., Hannan M. A., Karim T. F., Hussain A., Saad M. H. M., Ayob A., Miah M. S., Indra Mahlia T. M., Intelligent algorithms and control strategies for battery management system in electric vehicles: Progress, challenges and future outlook. *Journal of Cleaner Production* 292, 126044, 2021. <https://doi.org/10.1016/j.jclepro.2021.126044>.
- Jin Y., Zhao W., Li Z., Liu B., Wang K., SOC estimation of lithium-ion battery considering the influence of discharge rate. *Energy Reports* 7(7), 1436-1446, 2021. <https://doi.org/10.1016/J.EGYR.2021.09.099>.
- Kuchly J., Goussian A., Merveillaut M., Baghdadi I., Franger S., Nelson-Gruel D., Nouillant C., Chamailard Y., Li-ion battery SOC estimation method using a Neural Network trained with data generated by a P2D model, *IFAC-PapersOnLine* 54(10), 336-343, 2021. <https://doi.org/10.1016/J.IFACOL.2021.10.185>.
- Li Y., Chattopadhyay P., Xiong S., Ray A., Rahn C.D., Dynamic data-driven and model-based recursive analysis for estimation of battery state-of-charge. *Applied Energy* 184, 266-275, 2016. <http://dx.doi.org/10.1016/j.apenergy.2016.10.025>
- Li X., Zhang L., Wang Z., Dong P., Remaining useful life prediction for lithium-ion batteries based on a hybrid model combining the long short-term memory and Elman neural networks. *Journal of Energy Storage* 21, 510-518, 2018. <https://doi.org/10.1016/j.est.2018.12.011>.
- Liu Q., Yu Q., The lithium battery SOC estimation on square root unscented Kalman filter, *Energy Reports* 8(7), 286–294, 2022. <https://doi.org/10.1016/J.EGYR.2022.05.079>.
- Lv J., Wang X., Wang G., Song Y., Research on Control Strategy of Isolated DC Microgrid Based on SOC of Energy Storage System. *Electronics* 10(7), 834, 2021. <https://doi.org/10.3390/ELECTRONICS10070834>.

- Okay K., Eray S., Eray A., Development of prototype battery management system for PV system. *Renew Energy* 181,1294-1304, 2022. <https://doi.org/10.1016/J.RENENE.2021.09.118>.
- Ren H., Zhao Y., Chen S., Wang T., Design and implementation of a battery management system with active charge balance based on the SOC and SOH online estimation. *Energy* 166, 908-917, 2019. <https://doi.org/10.1016/J.ENERGY.2018.10.133>.
- Shen Z, Rahn C. Model-based state-of-charge estimation for a valve-regulated lead-acid battery using matrix inequalities. *Journal of Dynamic Systems, Measurement, and Control* 135(4), 041015, 2018. <https://doi.org/10.1115/1.4023766>
- Singh K. V., Bansal H. O., Singh D., Hardware-in-the-loop Implementation of ANFIS based Adaptive SoC Estimation of Lithium-ion Battery for Hybrid Vehicle Applications, *Journal of Energy Storage* 27, 101124, 2020. <https://doi.org/10.1016/J.EST.2019.101124>.
- Somasundaram P., Jegadheesan C., Pal Singh A., Vivekanandhan C., Suganth S., Vikaash R., Shankarguru E., Effect of ambient pressure on charging and discharging characteristics of lead acid battery. *Materials Today Proceedings* 64(1), 888-894 2022. <https://doi.org/10.1016/J.MATPR.2022.05.401>.
- Tawalbeh M., Murtaza S. Z. M., Al-Othman A., Alami A. H., Singh K., Olabi A. G., Ammonia: A versatile candidate for the use in energy storage systems. *Renewable Energy* 194, 955-977, 2022. <https://doi.org/10.1016/j.renene.2022.06.015>
- Wang S., Fernandez C., Shang L., Li Z., Li J., Online state of charge estimation for the aerial lithium-ion battery packs based on the improved extended Kalman filter method. *Journal of Energy Storage*, 9, 69-83, 2017. <http://dx.doi.org/10.1016/j.est.2016.09.008>
- Wu Y., Zhao H., Wang Y., Li R., Zhou Y., Research on life cycle SOC estimation method of lithium-ion battery oriented to decoupling temperature. *Energy Reports* 8, 4182-4195, 2022. <https://doi.org/10.1016/J.EGYR.2022.03.036>.
- Zhang Y., Yang G., Ma S., Non-intrusive load monitoring based on convolutional neural network with differential input. *Procedia CIRP*, 83, 670-674, 2019. <https://doi.org/10.1016/j.procir.2019.04.110>.
- Zhao X., Xuan D., Zhao K., Li Z., Elman neural network using ant colony optimization algorithm for estimating of state of charge of lithium-ion battery. *Journal of Energy Storage* 32, 101789, 2020. <https://doi.org/10.1016/j.est.2020.101789>.